Published in final edited form as:
*Biochemistry*. 2012 July 10; 51(27): 5486–5495. doi:10.1021/bi3006048.

# Mechanism of inhibition of the glutamate transporter EAAC1 by the conformationally-constrained glutamate analog (+)-HIP-B

**Randolph Callender**[1], **Armanda Gameiro**[1], **Andrea Pinto**[2], **Carlo DeMicheli**[2], and **Christof Grewer**[1,*]

[1]Department of Chemistry, Binghamton University, Binghamton, NY 13902

[2]Dipartimento di Scienze Farmaceutiche, Università degli Studi di Milano, 20133 Milano, Italy

## Abstract

Glutamate transporters play an important role in the regulation of extracellular glutamate concentrations in the mammalian brain and are, thus, promising targets for therapeutics. Despite this importance, the development of pharmacological tools has mainly focused on the synthesis of competitive inhibitors, which are amino acid analogs that bind to the substrate binding site. In this report, we describe the characterization of the mechanism of glutamate transporter inhibition by a constrained, cyclic glutamate analog, (+)-3-Hydroxy-4,5,6,6a-tetrahydro-3a*H*-pyrrolo[3,4-*d*]isoxazole-6-carboxylic acid [(+)-(3aS,6S,6aS)-HIP-B]. Our results show that (+)-HIP-B is a non-transportable amino acid that inhibits glutamate transporter function in a mixed mechanism. Although (+)-HIP-B inhibits the glutamate-associated anion conductance, it has no effect on the leak anion conductance, in contrast to competitive inhibitors. Furthermore, (+)-HIP-B is unable to alleviate the effect of the competitive inhibitor DL-*threo*-β-Benzyloxyaspartic acid (TBOA), which binds to the substrate binding site. (+)-HIP-B is more potent in inhibiting forward transport compared to reverse transport. In a mutant transporter, which is activated by glutamine, but not glutamate, (+)-HIP-B still acts as an inhibitor, although this mutant transporter is insensitive to TBOA. Finally, we analyzed the effect of (+)-HIP-B on the pre-steady-state kinetics of the glutamate transporter. The results can be explained with a mixed mechanism at a site that may be distinct from the substrate binding site, with a preference for the inward-facing configuration of the transporter and slow inhibitor binding. (+)-HIP-B may represent a new paradigm of glutamate transporter inhibition that is based on targeting of a regulatory site.

Glutamate is the major excitatory neurotransmitter in the mammalian brain (reviewed in (1)). It mediates synaptic signal transmission by binding to and activating postsynaptic ionotropic and metabotropic glutamate receptors. After completion of the signal transmission process, glutamate is removed from the synapse by (i) passive diffusion (2) and (ii) active transport into neurons and adjacent glial cells (3). Reuptake of glutamate is mediated by high affinity transporters that reside in the plasma membrane, and it is energetically driven by the concentration gradients for sodium and potassium across the membrane (4–7).

The pharmacology of glutamate transporters has been studied in significant detail (8–10). A large number of amino acid analogues have been identified that displace glutamate from its binding site, acting as competitive inhibitors (8–10). Among the more frequently used compounds is DL-*threo*-β-benzyloxyaspartic acid (TBOA), which is a non-transportable aspartate analogue and inhibits glutamate transport with high apparent affinity in the sub-

*Address correspondence to: Christof Grewer, PhD, Department of Chemistry, Binghamton University, 4400 Vestal Parkway East, Binghamton, NY 13902, Phone: (607) 777-3250, Fax: (607) 777-4478, cgrewer@binghamton.edu..

μM range (10). Based on the identified pharmacophore, which contains a large, hydrophobic group attached to the oxygen of hydroxyaspartate, several other blockers were designed with even higher inhibitory potency (11). Another glutamate analogue with a constrained bicyclic conformation is (±)-HIP-B (12–13). As compared to TBOA, which is neurotoxic, (±)-HIP-B displays very little neurotoxicity under physiological conditions (13). Subsequently, the preparation of the enantiopure forms of (±)-HIP-B was accomplished through an efficient synthetic procedure (14). The pair of enantiomers (+)-HIP-B/(−)-HIP-B were investigated for their ability to inhibit [$^3$H]D-aspartate uptake; (+)-HIP-B, characterized by the (*S*)-configuration at the amino acid stereogenic center, turned out to be the eutomer with an eudismic ratio equal to 10 (14). When compared to other EAAT blockers, HIP-B resembles a restricted conformation of both AMPA (2-amino-3-(5-methyl-3-oxo-1,2-oxazol-4-yl)propanoic acid) and kainic acid. Interestingly, initial inhibition studies suggested that HIP-B action is based on a non-competitive inhibition mechanism (13–14). This finding is surprising, because the structure of the compound would suggest interaction with the substrate binding site. However, detailed investigations of the inhibition mechanism have not been carried out.

This study focuses on the mechanism of inhibition of the excitatory amino acid carrier 1 (EAAC1) by (+)-HIP-B at steady state, as well as using rapid application of substrates by laser-photolysis of caged glutamate to analyze the pre-steady state kinetics. The effect of glutamate concentration on the inhibition constant, $K_i$, was consistent with a mixed inhibition mechanism. Furthermore, (+)-HIP-B was unable to alleviate the effect of the competitive inhibitor TBOA. Finally, (+)-HIP-B was able to inhibit a mutant glutamate transporter that binds glutamine rather than glutamate, while the competitive inhibitor TBOA was not able to inhibit this transporter. Pre-steady-state kinetic analysis suggested that substrate displacement is not necessary to explain the effects on transport current kinetics. Together, our results indicate that (+)-HIP-B is a slowly-dissociating inhibitor of glutamate transport by EAAC1 that operates through a mixed mechanism. We propose a detailed inhibitory mechanism that explains the experimental data. The structures of glutamate, glutamine, TBOA and (+)-HIP-B are shown in scheme 1:

## Experimental Procedures

### Materials

Amino acid (−)-**HIP-B** was prepared following the previously reported procedure (14). The chemical purity of (−)-**HIP-B** was secured by HPLC while the enantiomeric excess, evaluated by chiral HPLC under the following conditions: column, CHIROBIOTIC TAG, Astec; eluent, 50 mM $NH_4OAc$ in (EtOH–MeOH 3:2)/water 4:1 (v/v) with 0.1% acetic acid; flow rate, 1.00 mL/min., turned out to be e.e. >99.5%.

### Cell Culture and Expression of EAAC1

HEK 293T cells (ATCC No. CRL 1573) were transfected using the JetPRIME DNA transfection reagent (PolyPlus Transfection) at a concentration of 0.25 μg plasmid DNA and 0.25 μg Red Fluorescent Protein DNA for 3.0 μL of JetPRIME. The incubation period post-transfection was at least twenty four hours before experiments were performed. Cells were cultured as previously described (15).

### Electrophysiology

Whole-cell current recording experiments were performed using an Adams and List patch clamp amplifier L/M-EPC7. Solution exchange and voltage Protocols were implemented using Clampex 7 software (Axon Instruments).

For experiments under forward transport conditions, the extracellular solution contained 140 mM NaMES (MES = methanesulfonic acid), 2 mM $MgCl_2$, 2 mM $CaCl_2$ and 10 mM HEPES (pH 7.35); the pipette solution contained 140 mM KMES, 2 mM $MgCl_2$, 10 mM EGTA and 10 mM HEPES (pH 7.4). For reverse transport, KMES was used extracellularly and NaMES in the pipette solution. In both forward and reverse transport experiments, L-glutamate was applied extracellularly. For homoexchange conditions, an extracellular solution containing 140 mM NaCl and a saturating concentration of 1mM L-glutamate was used (16). The pipette solution contained 140 mM NaSCN and 10 mM L-glutamate.

### Laser Pulse Photolysis

Laser pulse photolysis was accomplished using the high energy Q-switched Nd:YAG laser MiniLite II (Continuum Electro-Optics, Inc.). Energy density was approximately 300 mJ/$cm^2$. An optical fiber was used to transmit laser light to the patch clamp setup. Neutral density filters with absorption of 0.10 and 0.35 were placed in the optical path to control the energy transmitted and, correspondingly, the concentration of L-glutamate released during the experiment. 4-Methoxy-7-nitroindolinyl-caged-L-glutamate, MNI glutamate (17), was obtained from Tocris (Cat. No. 1490) and prepared at 1–2 mM concentrations. Once triggered, the approximately 5 ns laser pulse at 355 nm photolyzed the caged compound and free L-glutamate was released with a half time of about 200 ns (17). The 0.10 and 0.35 filters correspond to approximately 100 μM and 60 μM of released L-glutamate, respectively. The specific Clampex 7 laser protocol used consisted of a four-second pre-incubation period with MNI-caged-L-glutamate followed by the 5 ns laser pulse and finally 160 ms of pre-steady state data sampled at 50 kHz.

### Data Analysis

Experimental data was fit using a standard exponential function in Clampfit 9.2 (Axon Instruments) and graphed using Origin 7 software (OriginLab). For the transport current, the data was fit using a three-term exponential function. The one rise and two decay time constants were then converted into relaxation rate constants. The two decay relaxation rate constants were identified with distinct fast and slow decay processes, as described previously (18).

## Results

### (+)-HIP-B is not transported by the glutamate transporter and does not activate the anion conductance

Since the (+)-HIP-B structure contains elements of the glutamate scaffold, it is possible that it can be transported by the glutamate transporter EAAC1. To test this possibility, we measured whole cell currents in the presence of (+)-HIP-B. As shown in Fig. 1A, application of 100 μM glutamate to EAAC1 induced inward current in the presence of intracellular $SCN^-$, due to the activation of $SCN^-$ outflow. Under the same conditions, the competitive inhibitor TBOA generated outward current (Fig. 1B), caused by the well established inhibition of the tonic leak anion conductance (15). Surprisingly, (+)-HIP-B did not induce or inhibit anion current (Fig. 1C). In the absence of permeable intracellular anion, the transport component of the current can be observed. Consistent with previous reports (15–16), glutamate, as a transported substrate, induced inward transport current when applied to EAAC1 at a concentration of 100 μM (Fig. 1D). In contrast, (+)-HIP-B did not elicit transport current (Fig. 1E), indicating that it is not a transportable substrate for EAAC1, or that its transport rate is so low that it cannot be detected in our current recording assay. The data are quantified in Fig. 1F.

### (+)-HIP-B inhibits EAAC1 based on a mixed inhibition mechanism

(+)-HIP-B inhibited glutamate-induced anion currents in a concentration-dependent manner (Fig. 2A). These currents were recorded in the forward mode of transport, in which glutamate is transported into the cell. Upon reversing the ionic concentration gradient, the effect of (+)-HIP-B on the reverse transport mode was studied, in which glutamate is released from the cell. As shown in Fig. 2B, (+)-HIP-B also inhibited reverse transport current in the μM concentration range.

To identify the mechanism of inhibition, we determined the inhibition constant, $K_i$, at three different glutamate concentrations. Here, and throughout the manuscript, we will discuss results mainly by comparison with a competitive mechanism, which is the expected mechanism based on the structural similarities between transported substrates and HIP-B. As shown in Fig. 2C, the inhibition constant of 8.7 ± 1.5 μM (n = 3) at 20 μM glutamate increased only slightly to 9.2 ± 1.2 μM (n = 3) when [glutamate] was increased to 100 μM, indicating that inhibition is not purely competitive. The expected [glutamate] dependence for simple competitive inhibition is shown in Fig. 2D, calculated according to equation 1:

$$K_i = K_i(0)\,[1 + [\mathrm{Glu}]/K_m] \quad \text{(eq. 1)}$$

Here, $K_i(0)$ is the inhibition constant of (+)-HIP-B in the absence of glutamate, and $K_m$ is the apparent affinity of the transporter for glutamate. The experimental $K_i$ under transport conditions (not shown in Fig.2D) mirrors the $K_i$ under anionic conditions (shown in Fig. 2D), albeit at a lower concentration. The results demonstrate that the inhibition data cannot be explained with a purely competitive mechanism, in agreement with previous results (13, 19).

Next, we determined the $K_i$ for (+)-HIP-B in the $Na^+$/glutamate exchange mode, as well as in the reverse transport mode. In the exchange mode, the transporter is restricted to states in the transport cycle that are associated with glutamate translocation (16). Anion currents associated with exchange were inhibited with a $K_i$ of 19.0 ± 3.3 μM (n = 3) at 20 μM glutamate (Fig. 2E). Like in the forward transport mode, the inhibition constant increased only slightly with increasing glutamate concentrations, suggesting mixed inhibition. The inhibition constant in the reverse transport mode, in which the transporter binding sites should be mainly facing the extracellular solution, was higher with a value of 23.2 ± 2.5 μM (n = 3) at 20 μM glutamate (Fig. 2E). Together, these data suggest that (+)-HIP-B preferentially interacts with the inward-facing configuration of the transporter, which is mainly populated in the forward transport mode.

### (+)-HIP-B does not alleviate the effects of the competitive inhibitor TBOA

TBOA is a well known, non-transportable and competitive inhibitor of glutamate transport (10). It binds at the glutamate binding site and also inhibits the leak anion current (15). In contrast to TBOA, (+)-HIP-B is unable to inhibit leak anion current (Fig. 1). If displacement occurs, TBOA inhibition of leak anion current would be alleviated by (+)-HIP-B, indicating that (+)-HIP-B binds to the TBOA binding site. As expected, TBOA inhibited the leak anion current, which is manifested as an outward current due to inhibition of the persistent inward anion current in the presence of intracellular $SCN^-$ (10). Application of 30 μM (+)-HIP-B alone elicited no response (Fig. 3A, middle panel). When TBOA (1 μM) was applied in the presence of (+)-HIP-B, the TBOA-induced outward current was not inhibited (Fig. 3A, right panel). 1 μM TBOA is a concentration that is two-fold $K_i$ (10, 15). (+)-HIP-B seems unable to alleviate the TBOA effect at any concentration tested (up to 70 μM, which is well beyond the $K_i$ of EAAC1 for (+)-HIP-B, Fig. 2). Together, these results indicate that TBOA and (+)-HIP-B are not competing for the same binding site on EAAC1.

### (+)-HIP-B inhibits a mutant glutamate transporter that does not bind glutamate

Substrate binding by $EAAC1_{WT}$ requires negative charge of the γ-carboxylate group of the transported substrate, glutamate (20–21). Once bound, the negative charge of the γ-carboxylate is presumably ion-paired with a positively-charged guanidinium group of arginine 446 (22), which is highly conserved in glutamate transporters. Therefore, we examined if (+)- HIP-B could inhibit the function of EAAC1 with the R446Q mutation, which binds neutral amino acids instead of acidic amino acids (22). If the mechanism of inhibition is competitive, it would be expected that HIP-B would not bind to the mutant transporter, due to its inability to establish salt bridge interaction with R446Q. As controls, we compared the currents induced by L-glutamine to those induced by L-glutamate and TBOA (Figs. 4A, D and E). While glutamine elicited significant anion current, insignificant currents of < 5 pA were observed upon application of glutamate and TBOA. According to the p$K_a$ of (+)-HIP-B (5.1, (12)), the 3-hydroxyl-$\Delta^2$-isoxazoline group should also be negatively charged, suggesting that (+)-HIP-B would be unable to interact with the R446Q mutant transporter. In contrast to this expectation, the application of successive amounts of (+)-HIP-B (10 and 50 μM in the presence of 50 μM L-glutamine) showed increasing inhibition, indicating that (+)-HIP-B does not interact with the substrate binding site, as was shown for the wild type transporter (Fig. 4A). The apparent $K_i$ for of $EAAC1_{R446Q}$ inhibition by (+)-HIP-B was determined by extrapolating the linear dependence of the $K_i$ as a function of the concentration to 0 mM (+)-HIP-B as $K_i$ = 2.8 ± 1.6 μM (Fig. 4B). These data indicates that (+)-HIP-B inhibits the mutant transporter with a higher apparent affinity than wild type EAAC1 (Fig. 4C).

### (+)-HIP-B dissociates slowly from its binding site

The next question was whether (+)-HIP-B interaction with its transporter binding site is slow or fast. To answer this question, we performed pre-incubation experiments, in which (+)-HIP-B was applied to the transporter by solution exchange for 2 seconds, followed by rapid washout and application of a super-saturating glutamate concentration at the same time (Fig. 5). We used a super-saturating glutamate concentration to allow for the detection of fast activation kinetics under conditions of solution exchange with a 10 ms time resolution. As shown in Fig. 5A, left panel, the time constant for activation of anion current by glutamate was 7 ± 2 ms. The intrinsic time constant for this activation process is in the 1 ms range, suggesting that solution exchange is rate limiting with a time constant in the 10 ms range. When 1 mM glutamate was applied after preincubation with 20 mM (+)-HIPB (Fig. 5A, middle panel), activation of the anion current was significantly slowed, with a time constant of 55 ± 1 ms. This time constant is 5-fold slower than the solution exchange time, indicating that it reflects the kinetics of (+)-HIP-B dissociation from its EAAC1 binding site. Furthermore, this time constant was not significantly affected by the pre-applied (+)-HIP-B concentration (Figs. 5A, right panel, and 5C). The (+)-HIP-B effect was completely reversible, as shown in Fig. 5B. Slowing of glutamate-induced anion current activation can be explained by a rate-limiting (+)-HIP-B dissociation process. Here, (+)-HIP-B has to dissociate from the transporter first, before current is observed. This phenomenon can be described by the following equation for the observed relaxation rate constant, $k_{obs}$:

$$k_{obs}=k_d+k_f\,[I] \quad \text{(eq. 2)}$$

Here, $k_d$ is the rate constant for (+)-HIP-B dissociation and $k_f$ is the rate constant for (+)-HIP-B binding. In the case of (+)-HIP-B concentration ([I]) = 0 used in the washout experiment, this equation reduces to $k_{obs} = k_d$. Therefore, the observed dissociation rate constant is expected to be independent of the pre-applied [(+)-HIP-B], consistent with the experimental data (Fig. 5C). Together, these data suggest that (+)-HIP-B dissociation from its binding site is slow, occurring on a time scale of 50 – 60 ms.

### Lack of effect of (+)-HIP-B on pre-steady-state kinetics

The analysis of transient kinetics provides a powerful tool for the determination of the mechanism of inhibition of membrane proteins (23–24). In order to obtain data with a sub-millisecond time resolution, we applied glutamate through photolysis of a caged precursor, MNI-caged glutamate. It was shown previously that photolysis occurs with a time constant of 0.2 μs (17). Both forward anion conducting (Figs. 6C and D) and transport modes (Figs. 6A and B) were studied. When glutamate was applied in the forward transport mode, a rapidly-decaying transient current was observed, which precedes steady-state transport (Fig. 6A). Consistent with previous reports (15, 18), this transient current decayed with two exponential components. The two phases are linked to the glutamate translocation process (15, 18). In the presence of (+)-HIP-B, the peak current was inhibited (Fig. 6B). However, the two time constants, $\tau_{fast}$ and $\tau_{slow}$, representing the two component decay to steady-state, were virtually unaffected by the presence of the inhibitor (Fig. 6). Furthermore, the rate constant for the rise of the transport current, which was previously associated with glutamate binding, was not dependent on [(+)-HIP-B]. If inhibition was rapid and competitive, it would be expected that increasing (+)-HIP-B concentrations would successively slow glutamate binding, according to the following equation for the observed binding rate constant, $k_{obs}$(Glu binding):

$$k_{obs}\,(\text{Glu binding}) = k_b{}^{*} K_i \,/\, (K_i + [\text{I}]) \quad \text{(eq. 3)}$$

Here, $k_b$ is the bimolecular rate constant for glutamate binding and [I] is the (+)-HIP-B concentration. Therefore, it is unlikely that HIP-B slows glutamate binding through a rapid, competitive displacement process.

In the case of the anion current, we observed that time constants $\tau_{rise}$ and $\tau_{slow}$, which represent activation of the anion conductance and the single-exponential decay to steady-state, were also independent of [(+)-HIP-B], within experimental error. Consistent with our observations for the transport component of the current, the peak of the transient current was inhibited strongly by (+)-HIP-B (Fig. 6).

The lack of an effect of (+)-HIP-B on the rate constant associated with relaxation of the pre-steady-state current was surprising, but can be explained assuming that the interaction of the inhibitor with EAAC1 is slow compared to the relaxation of the transient current, according to the following kinetic scheme:

According to this concept, the inhibitor-bound forms of the transporter, $IT_o$ and $IT_oGlu$ interconvert with the non-inhibitor-bound forms ($T_o$ and $T_oGlu$) on a slower timescale compared to translocation (characterized by $k_t$ in the absence and $k_t$(I) in the presence of (+)-HIP-B). The relaxation will then consist of two exponential components. However, since $k_t$(I) is expected to be much smaller than $k_t$, only the non-inhibited component is observed, which decays with the native time observed constant that is the same as in the absence of (+)-HIP-B. However, the peak current is inhibited, as the inclusion of the inhibitor has essentially the same effect as a reduction of the number of active transporters under observation:

$$I_t \approx k_t \frac{[\text{Glu}]}{[\text{Glu}] + K_m} \frac{K_i}{[\text{I}] + K_i} + k_t\,(\text{I}) \frac{[\text{Glu}]}{[\text{Glu}] + K_m} \frac{[\text{I}]}{[\text{I}] + K_i} \quad \text{(eq. 4)}$$

This equation reduces to

$$I_t \approx k_t \frac{[Glu]}{[Glu]+K_m} \frac{K_i}{[I]+K_i} \qquad \text{for } k_t \gg k_t(I) \quad \text{(eq. 5)}$$

in case of slow translocation in the inhibitor-bound state. Eq. 4 represents the observed inhibition data at steady-state well (Figs. 2 and 6).

## Discussion

This report identifies mechanistic aspects of the inhibition of the neuronal glutamate transporter subtype EAAC1 by the conformationally-restrained glutamate analogue (+)-HIP-B. The p$K_a$ value of the 3-hydroxyl-$\Delta^2$-isoxazoline group of (+)-HIP-B is 5.1 (12). Thus, this group should be predominantly deprotonated at physiological pH, indicating it is negatively charged. Therefore, it was expected that (+)-HIP-B would be isosteric to glutamate, binding to the glutamate binding site and behaving as a competitive inhibitor, despite the contrary preliminary evidence reported by Funicello et al. (13).

Our detailed mechanistic analysis clearly demonstrates that (+)-HIP-B inhibition of EAAC1 cannot be explained with a purely competitive mechanism with fast inhibitor binding and dissociation. This conclusion is based on several experimental findings: 1) The weak dependence of the $K_i$ for (+)-HIP-B of the glutamate concentration (Figs. 2D and E). If the mechanism would be purely competitive, we would expect that (+)-HIP-B inhibition should be overcome at high glutamate concentrations. However, this was not the case (Fig. 2D). 2) The inability of (+)-HIP-B to alleviate the effects of the competitive blocker TBOA (Fig. 3B). 3) The inhibition of EAAC1 with the R446Q mutation, which at physiological pH binds neutral amino acids, but not acidic amino acids, such as glutamate. If the negatively-charged (+)-HIP-B would inhibit by competitively binding only to the substrate binding site, it would be expected that $EAAC1_{R446Q}$ function would not be inhibited by (+)-HIP-B, because the ion pair interaction of the negative side chain group and the positively-charged arginine are necessary for binding to the transporter. This ion pair interaction is disrupted in $EAAC1_{R446Q}$, but (+)-HIP-B still binds with even better apparent affinity as to the wild-type transporter. At least a dramatic reduction in apparent affinity of the $EAAC1_{R446Q}$ compared to the wild-type transporter would be expected, as less than 1% of (+)-HIP-B should be in its neutral form at pH 7.3, based on its p$K_a$. 4) Although the affinity of $EAAC1_{R446Q}$ for (+)-HIP-B is slightly reduced at high glutamate concentrations, interaction of (+)-HIP-B with $EAAC1_{R446Q}$ is not consistent with a pure competitive mechanism, as shown in Fig. 4. Taken together, these results suggest that (+)-HIP-B inhibits EAAC1 through a mixed mechanism that is mainly non-competitive, but also shows some aspects of competitive inhibition due to the slight increase of the $K_i$ for (+)-HIP-B with increasing [substrate]. Therefore, the possibility must be considered that (+)-HIP-B binds to an allosteric site on the glutamate transporter, despite its structural similarity with transported substrates.

If purely competitive inhibition is not compatible with the data, the next question has to be what type of inhibition mechanism can account for the results. From the low dependence of the apparent $K_i$ for (+)-HIP-B on the glutamate concentration, it is evident that such a mechanism has to include binding of the inhibitor to both the empty transporter, as well as to the glutamate-bound form of EAAC1. However, a simple mixed inhibition mechanism, in which inhibitor association is fast compared to the conformational changes of the transporter, is not consistent with the pre-steady-state kinetic results (Fig. 6), which show that the relaxation rates are independent of the (+)-HIP-B concentration. For the mixed mechanism, it would be expected that these relaxation rates decrease with increasing inhibitor concentration. In order to account for these data, the assumption has to be made that inhibitor interaction with EAAC1 is slow compared to the glutamate translocation

process in the absence of (+)-HIP-B. This assumption is supported by the experimental data, showing that dissociation of (+)-HIP-B takes place on the 50 ms time scale. With a $K_i$ value in the 20 μM range, a bimolecular rate constant for (+)-HIP-B binding in the range of $10^6$ $M^{-1}s^{-1}$ can be estimated, indicating that binding at the relevant concentration range occurs on a 20–50 ms time scale. In contrast, the steps associated with glutamate translocation were shown to have time constants of 8 ms and smaller. Therefore, the assumption of slow inhibitor binding/dissociation seems to be justified.

Overall, we propose a kinetic mechanism for inhibition that is illustrated in Fig. 7. In this mechanism, (+)-HIP-B slowly binds to a modulatory site, altering the intrinsic rate constants associated with cycling through the distinct states in the transport cycle. (+)-HIP-B most likely has a predominant effect on the rate constants for glutamate translocation, with a lesser effect on the rate constant for relocation of the $K^+$-bound transporter. The reason for this conclusion is that at intermediate concentrations, (+)-HIP-B inhibits the transient component of the transport current, which is associated with translocation, more strongly than the steady-state component, which is rate limited by $K^+$-induced transporter relocation (15, 25). Our results in the homo-exchange and reverse transport modes suggest that the inward facing configuration is slightly preferred by (+)-HIP-B, but that it can also interact with the outward-facing configuration, although with slightly lower affinity.

(+)-HIP-B has been investigated regarding its ability to interact with glutamate transporters in synaptosomes prepared from rat brains (13–14). (+)-HIP-B was found to inhibit glutamate uptake, consistent with the results obtained here. (+)-HIP-B also inhibited aspartate release, which was induced by glutamate application (exchange-mediated release, (13)). Consistently, we show that (+)-HIP-B inhibits currents in the glutamate homo-exchange mode. It is not precisely known which glutamate transporter subtypes were present in the synaptosomal preparation, although the sensitivity to dihydrokainate (DHK) suggests that EAAT2 was the predominant transporter (13). Therefore, results may vary slightly between the Funicello et al. report (13) and our results, because (+)-HIP-B's effects may be subtype dependent. One interesting aspect is that (+)-HIP-B was able to elicit some aspartate release in synaptosomes, although to a much smaller extent that glutamate (13). This suggests that (+)-HIP-B is a partial substrate in this preparation. In contrast, we did not find any substrate activity, assuming that (+)-HIP-B transport, if possible, would be electrogenic. It is, however, possible that other glutamate transporter subtypes transport (+)-HIP-B at high concentrations and low rates, thus promoting at least some aspartate release through exchange.

Our results clearly demonstrate that (+)-HIP-B inhibits both transport activity, as well as the glutamate-dependent anion conductance. In contrast to all other competitive blockers investigated so far, (+)-HIP-B has no effect on the leak anion conductance of the transporter. This finding indicates a different inhibition mechanism compared to other known blockers (10–11, 26–27), as also indicated by the mixed inhibition kinetics compared to purely competitive behavior for most of the known inhibitors. It was previously proposed for the (+)-HIP-B analogue (−)-HIP-A that inhibition becomes competitive when the compound is co-applied with the transported substrate, instead of being pre-incubated (14). Our data for (+)-HIP-B show that even upon co-application a mixed, or non-competitive inhibition mechanism is observed. In addition, our data did not show a slow effect of (+)-HIP-B in the time scale of minutes to hours, as inhibition was fully reversible within 500 ms.

Alteration of the glutamate transport rate through an allosteric site has been proposed for the potentiation of glutamate transport by a compound from spider venom, parawixin1 (28), as well as for inhibition by arachidonic acid (29). Parawixin1 enhances glutamate uptake by the subtype EAAT2 by a factor of about 1.5, by increasing the rate of $K^+$-induced transporter

relocation (28). In contrast to (+)-HIP-B, which is only moderately selective with respect of inhibition of the glutamate transporter subtypes, parawixin1 targets only EAAT2. Based on the different selectivities and inhibition mechanisms, (+)-HIP-B and parawixin1 most likely do not act at the same site. However, the parawixin1 and arachidonic acid results demonstrate precedence for the existence of regulatory sites on the glutamate transporter that can not only inhibit, but also enhance uptake. Therefore, allosteric modulation of the transport rate in both directions may be possible.

## Conclusions

By using several different approaches, our data show that (+)-HIP-B inhibition of the neuronal glutamate transporter EAAC1 cannot be explained by a purely competitive mechanism. A mechanism that is consistent with the experimental data includes binding of (+)-HIP-B to both the glutamate-bound and glutamate-free form of EAAC1, with slightly higher affinity to the empty transporter (*apo* state). Furthermore, inhibitor effect on the inward facing conformation seems to be stronger compared to the outward-facing configuration, a finding that also deviated from the expectations for a simple competitive mechanism. The possibility has to be considered that a regulatory site exists on glutamate transporters that allows inhibition based on a mixed mechanism. Existence of a regulatory site would open up new avenues for the development of therapeutic agents acting on glutamate transporters based on an allosteric mechanism.

## Acknowledgments

This work was supported by the National Institutes of Health Grant 2R01NS049335-06A1 awarded to CG, and a Binational Science Foundation (BSF), Grant 2007051 awarded to CG and B. I. Kanner. R. Callender is grateful for support through a Clark fellowship from the Binghamton University Graduate School. Financial support from the Italian Ministry of Education (MIUR, Rome – PRIN 2007E8CRF3_004) is gratefully acknowledged.

## Abbreviations

| | |
|---|---|
| **AMPA** | 2-amino-3-(5-methyl-3-oxo-1,2-oxazol-4-yl)propanoic acid |
| **EAAC1** | Excitatory amino acid carrier 1 |
| **EAAT** | Excitatory amino acid transporter |
| **(+)-HIP-B** | (+)-(3aS,6S,6aS)-3-Hydroxy-4,5,6,6a-tetrahydro-3aH-pyrrolo[3,4-d]isoxazole-6-carboxylic acid |
| **(−)-HIP-B** | (−)-(3aR,6R,6aR)-3-Hydroxy-4,5,6,6a-tetrahydro-3aH-pyrrolo[3,4-d]isoxazole-6-carboxylic acid |
| **(−)-HIP-A** | (−)-(3aR,4S,6aR)-3-Hydroxy-4,5,6,6a-tetrahydro-3a H-pyrrolo[3,4-d]isoxazole-4-carboxylic acid |
| **TBOA** | DL-*threo*-β–benzyloxyaspartate |
| **EGTA** | Ethylene glycol-bis(2-aminoethylether)-*N,N,N′,N′*-tetraacetic acid |
| **HEK** | Human embryonic kidney |
| **HEPES** | 4-(2-Hydroxyethyl)piperazine-1-ethanesulfonic acid |
| **MES** | Methanesulfonate |
| **MNI-glutamate** | 4-Methoxy-7-nitroindolinyl-caged-L-glutamate |
| **Glu** | Glutamate |

| | |
|---|---|
| **I** | Inhibitor |
| **T** | Transporter |

## References


1. Kandel, ER.; Schwartz, JH.; Jessell, TM. Essentials of Neural Science and Behavior. Appleton & Lange; 1995.
2. Clements JD. Transmitter timecourse in the synaptic cleft: its role in central synaptic function. Trends Neurosci. 1996; 19:163–171. [PubMed: 8723198]
3. Diamond JS, Jahr CE. Transporters buffer synaptically released glutamate on a submillisecond time scale. J Neurosci. 1997; 17:4672–4687. [PubMed: 9169528]
4. Kanai Y, Hediger MA. Primary structure and functional characterization of a high-affinity glutamate transporter. Nature. 1992; 360:467–471. [PubMed: 1280334]
5. Kanner BI, Sharon I. Active transport of L-glutamate by membrane vesicles isolated from rat brain. Biochemistry. 1978; 17:3949–3953. [PubMed: 708689]
6. Pines G, Danbolt NC, Bjoras M, Zhang Y, Bendahan A, Eide L, Koepsell H, Storm-Mathisen J, Seeberg E, Kanner BI. Cloning and expression of a rat brain L-glutamate transporter. Nature. 1992; 360:464–467. [PubMed: 1448170]
7. Storck T, Schulte S, Hofmann K, Stoffel W. Structure, expression, and functional analysis of a Na(+)-dependent glutamate/aspartate transporter from rat brain. Proc Natl Acad Sci U S A. 1992; 89:10955–10959. [PubMed: 1279699]
8. Bridges RJ, Lovering FE, Koch H, Cotman CW, Chamberlin AR. A conformationally constrained competitive inhibitor of the sodium-dependent glutamate transporter in forebrain synaptosomes: L-anti-endo-3,4-methanopyrrolidine dicarboxylate. Neurosci Lett. 1994; 174:193–197. [PubMed: 7970177]
9. Luethi E, Nguyen KT, Burzle M, Blum LC, Suzuki Y, Hediger M, Reymond JL. Identification of selective norbornane-type aspartate analogue inhibitors of the glutamate transporter 1 (GLT-1) from the chemical universe generated database (GDB). J Med Chem. 2010; 53:7236–7250. [PubMed: 20812729]
10. Shimamoto K, Lebrun B, Yasuda-Kamatani Y, Sakaitani M, Shigeri Y, Yumoto N, Nakajima T. DL-threo-beta-benzyloxyaspartate, a potent blocker of excitatory amino acid transporters. Mol Pharmacol. 1998; 53:195–201. [PubMed: 9463476]
11. Shimamoto K. Glutamate transporter blockers for elucidation of the function of excitatory neurotransmission systems. Chem Rec. 2008; 8:182–199. [PubMed: 18563834]
12. Conti P, Dallanoce C, De Amici M, De Micheli C, Fruttero R. Synthesis of New Bicyclic Analogues of Glutamic Acid. Tetrahedron. 1999; 55:5623–5634.
13. Funicello M, Conti P, De Amici M, De Micheli C, Mennini T, Gobbi M. Dissociation of [3H]L-glutamate uptake from L-glutamate-induced [3H]D-aspartate release by 3-hydroxy-4,5,6,6a-tetrahydro-3aH-pyrrolo[3,4-d]isoxazole-4-carboxylic acid and 3-hydroxy-4,5,6,6a-tetrahydro-3aH-pyrrolo[3,4-d]isoxazole-6-carboxylic acid, two conformationally constrained aspartate and glutamate analogs. Mol Pharmacol. 2004; 66:522–529. [PubMed: 15322243]
14. Colleoni S, Jensen AA, Landucci E, Fumagalli E, Conti P, Pinto A, De Amici M, Pellegrini-Giampietro DE, De Micheli C, Mennini T, Gobbi M. Neuroprotective effects of the novel glutamate transporter inhibitor (−)-3-hydroxy-4,5,6,6a-tetrahydro-3aH-pyrrolo[3,4-d]-isoxazole-4-carboxylic acid, which preferentially inhibits reverse transport (glutamate release) compared with glutamate reuptake. J Pharmacol Exp Ther. 2008; 326:646–656. [PubMed: 18451317]
15. Grewer C, Watzke N, Wiessner M, Rauen T. Glutamate translocation of the neuronal glutamate transporter EAAC1 occurs within milliseconds. Proc Natl Acad Sci U S A. 2000; 97:9706–9711. [PubMed: 10931942]
16. Watzke N, Bamberg E, Grewer C. Early intermediates in the transport cycle of the neuronal excitatory amino acid carrier EAAC1. J Gen Physiol. 2001; 117:547–562. [PubMed: 11382805]

17. Canepari M, Nelson L, Papageorgiou G, Corrie JE, Ogden D. Photochemical and pharmacological evaluation of 7-nitroindolinyl-and 4-methoxy-7-nitroindolinyl-amino acids as novel, fast caged neurotransmitters. J Neurosci Methods. 2001; 112:29–42. [PubMed: 11640955]
18. Mim C, Tao Z, Grewer C. Two conformational changes are associated with glutamate translocation by the glutamate transporter EAAC1. Biochemistry. 2007; 46:9007–9018. [PubMed: 17630698]
19. Krause R, Watzke N, Kelety B, Dorner W, Fendler K. An automatic electrophysiological assay for the neuronal glutamate transporter mEAAC1. J Neurosci Methods. 2009; 177:131–141. [PubMed: 18996149]
20. Grewer C, Balani P, Weidenfeller C, Bartusel T, Tao Z, Rauen T. Individual subunits of the glutamate transporter EAAC1 homotrimer function independently of each other. Biochemistry. 2005; 44:11913–11923. [PubMed: 16128593]
21. Watzke N, Rauen T, Bamberg E, Grewer C. On the mechanism of proton transport by the neuronal excitatory amino acid carrier 1. J Gen Physiol. 2000; 116:609–622. [PubMed: 11055990]
22. Bendahan A, Armon A, Madani N, Kavanaugh MP, Kanner BI. Arginine 447 plays a pivotal role in substrate interactions in a neuronal glutamate transporter. J Biol Chem. 2000; 275:37436–37442. [PubMed: 10978338]
23. Grewer C, Rauen T. Electrogenic glutamate transporters in the CNS: molecular mechanism, pre-steady-state kinetics, and their impact on synaptic signaling. J Membr Biol. 2005; 203:1–20. [PubMed: 15834685]
24. Hess GP, Grewer C. Development and application of caged ligands for neurotransmitter receptors in transient kinetic and neuronal circuit mapping studies. Methods Enzymol. 1998; 291:443–473. [PubMed: 9661164]
25. Bergles DE, Tzingounis AV, Jahr CE. Comparison of coupled and uncoupled currents during glutamate uptake by GLT-1 transporters. J Neurosci. 2002; 22:10153–10162. [PubMed: 12451116]
26. Shimamoto K, Shigeri Y, Yasuda-Kamatani Y, Lebrun B, Yumoto N, Nakajima T. Syntheses of optically pure beta-hydroxyaspartate derivatives as glutamate transporter blockers. Bioorg Med Chem Lett. 2000; 10:2407–2410. [PubMed: 11078189]
27. Tsukada S, Iino M, Takayasu Y, Shimamoto K, Ozawa S. Effects of a novel glutamate transporter blocker, (2S, 3S)-3-[3-[4-(trifluoromethyl)benzoylamino]benzyloxy]aspartate (TFB-TBOA), on activities of hippocampal neurons. Neuropharmacology. 2005; 48:479–491. [PubMed: 15755476]
28. Fontana AC, de Oliveira Beleboni R, Wojewodzic MW, Ferreira Dos Santos W, Coutinho-Netto J, Grutle NJ, Watts SD, Danbolt NC, Amara SG. Enhancing glutamate transport: mechanism of action of Parawixin1, a neuroprotective compound from Parawixia bistriata spider venom. Mol Pharmacol. 2007; 72:1228–1237. [PubMed: 17646426]
29. Zerangue N, Arriza JL, Amara SG, Kavanaugh MP. Differential modulation of human glutamate transporter subtypes by arachidonic acid. J Biol Chem. 1995; 270:6433–6435. [PubMed: 7896776]

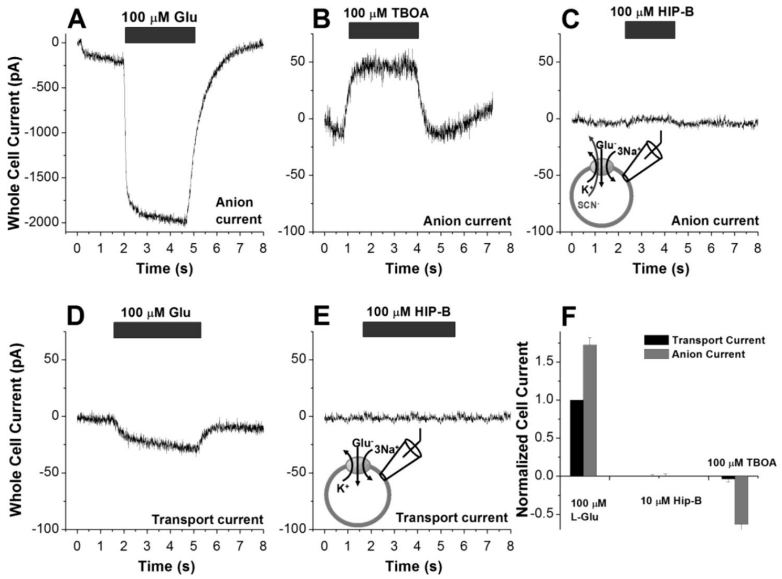


**Figure 1.**

(+)-HIP-B is not transported by the glutamate transporter and does not activate the anion conductance. **(A)** Original current trace with 100 μM L-glutamate applied in the anion conducting mode. **(B)** Original anion current trace induced by 100 μM TBOA. **(C)** 100 μM (+)-HIP-B did not induce or inhibit anion current. For (A–C) the extracellular solution contained 140 mM NaMES. The pipette solution contained 140 mM KSCN. The membrane potential was held at 0 mV. **(D)** Original current trace with 100 μM L-glutamate applied in the transport mode and 100 μM (+)-HIP-B applied **(E)**. Transport conditions were created using 140 mM NaMES in the extracellular solution and 140 mM KMES in the pipette solution. The membrane potential was held at 0 mV. **(F)** Average cell responses under ionic conditions favoring transport or anion current.

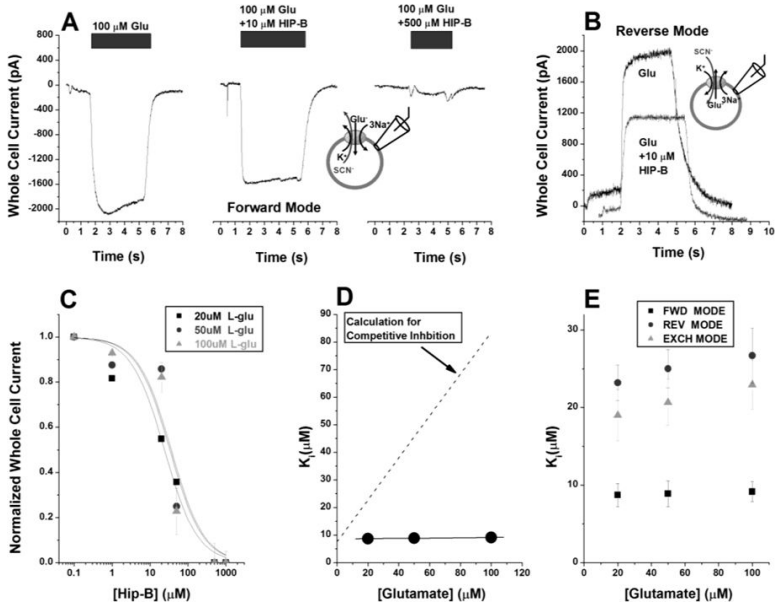


**Figure 2.**

(+)-HIP-B inhibits EAAC1 based on a mixed inhibition mechanism. **(A)** Three original traces recorded from $EAAC1_{WT}$ showing (+)-HIP-B's effects on L-glutamate-induced currents: 100 μM L-glutamate control (left), 100 μM L-glutamate + 10 μM (+)-HIP-B (middle) and 100 μM L-glutamate + 500 μM (+)-HIP-B (right). The extracellular solution contained 140 mM NaCl. The pipette solution contained 140 mM KSCN. The membrane potential is held at 0 mV. The small, transient currents at the time of solution exchange in the right panel are unspecific responses related to mechanical movement of the cell from switching of the pinch valves. **(B)** Two original current traces in the reverse transport mode with 100 μM TBOA in the absence and presence of 10 μM (+)-HIP-B. The conditions for reverse transport mode were 140 mM KSCN in the external solution and 140 mM NaCl + 10 mM L-Glu in the pipette solution. The 100 μM TBOA is applied externally. **(C)** Dose-response curves for (+)-HIP-B inhibition of $EAAC1_{WT}$ anion currents at glutamate concentrations of 20 μM (squares), 50 μM (circles) and 100 μM (triangles). The conditions are the same as in (A). The solid lines represent a fit to eq. 5. **(D)** The apparent $K_i$ for (+)-HIP-B in the forward transport mode a s a function of the L-glutamate concentration. As (+)-HIP-B alone does not elicit a response, the $K_i$ is extrapolated from the fit to zero L-glutamate concentration. The expected $K_i$ was calculated using the competitive inhibition equation $I(S) = K_i(0)+(K_i(0)/K_m)[\text{L-glu}]$ where $K_m$ is the apparent binding affinity for L-glutamate, $K_i(0)$ is the apparent $K_i$ for (+)-HIP-B and I is the current. **(E)** The apparent $K_i$ as a function of [glutamate] for (+)-HIP-B in the three EAAC1 transport modes: forward (square), reverse (circle) and homo-exchange (triangle). The conditions for the forward mode are the same as in (A). The conditions for reverse and homo-exchange modes are explained in the methods section.

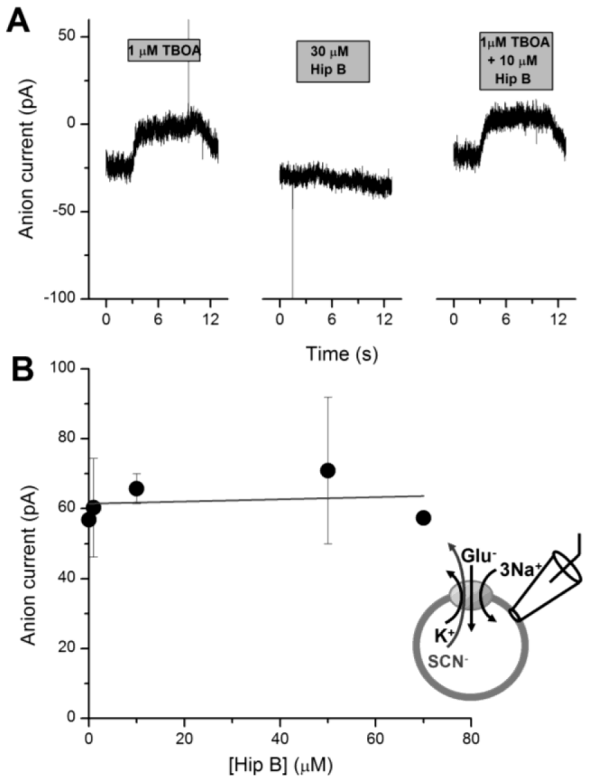


**Figure 3.**

(+)-HIP-B does not alleviate the effects of the competitive inhibitor TBOA. **(A)** Original traces of outward anion currents elicited by the application of TBOA alone (left trace) (+)-HIP-B alone (middle trace) and TBOA and (+)-HIP-B together (right trace) to $EAAC1_{WT}$. The timing and concentration are indicated by the gray bar. The membrane potential was 0 mV and the intracellular solution contained 120 mM KSCN. The extracellular solution contained 140 mM NaMes. **(B)** Application of (+)-HIP-B in increasing concentrations, in the presence of 1 μM TBOA. The results show no inhibition of the TBOA response by (+)-HIP-B. The experimental conditions are the same as in (A).

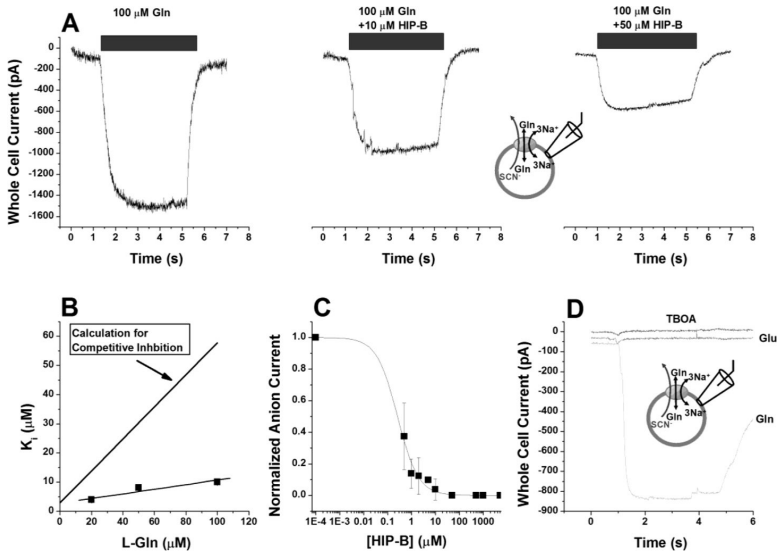


**Figure 4.**

(+)- HIP-B inhibits a mutant glutamate transporter that does not bind glutamate. **(A)** Three original current traces showing (+)-HIP-B's effects on L-glutamine-induced currents in EAAC1 with the R446Q mutation: 50 μM L-glutamine control (left), 50 μM L-glutamine + 10 μM (+)-HIP-B (middle) and 50 μM L-glutamine + 50 μM (+)-HIP-B (right). The extracellular solution contained 140 mM NaCl. The pipette solution contained 140 mM NaSCN and 10 mM L-glutamine. The membrane potential was held at 0 mV. **(B)** Determination of the apparent $K_i$ for R446Q in the exchange mode. The conditions are the same as in (A). The solid line was calculated for competitive inhibition according to Fig. legend 2. **(C)** Dose-response curve for the $EAAC1_{R446Q}$. 20 μM L-glutamine was used. The conditions are the same as in (A). The solid line represents a fit to eq. 5. **(D)** Application of 0.2 mM TBOA (black line) or 1 mM L-glutamate (light gray) did not induced currents in $EAAC1_{R446Q}$, in contrast to 0.5 mM L-alanine (dark gray). The pipette solution contained 140 mM NaSCN and 10 mM Ala. The extracellular solution contained 140 mM NaMES ($V_m$ = 0 mV).

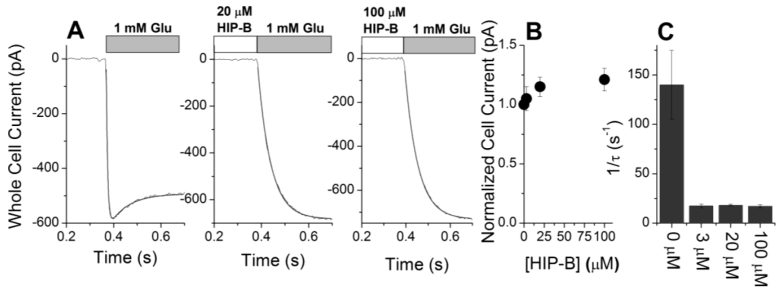


**Figure 5.**

(+)-HIP-B dissociation is slow compared to the rapid events in the transport cycle. **(A)** Rapid solution exchange from buffer only to buffer + 1 mM glutamate (left panel). In the middle and right panels, the cells were pre-incubated with 20 μM and 100 μM (+)-HIP-B, respectively, followed by a switch to 1 mM glutamate-containing solution. The extracellular solution contained 140 mM NaMES. The pipette solution contained 140 mM KSCN. The membrane potential was held at 0 mV. The pressure of the flow system was approximately 100 millibars, allowing solution exchange with a 10 ms time resolution. **(B)** Normalized cell responses (n = 3) using three (+)-HIP-B concentrations: 3, 20 and 100 μM with a 100 μM L-glutamate control, showing that the (+)-HIP-B effect is fully reversible. **(C)** Observed dissociation rate constants ($1/\tau$) in the presence of 0, 3, 20 and 100 μM (+)-HIP-B. The rate constant of the 1 mM L-glutamate control is determined by the rate of the solution exchange.

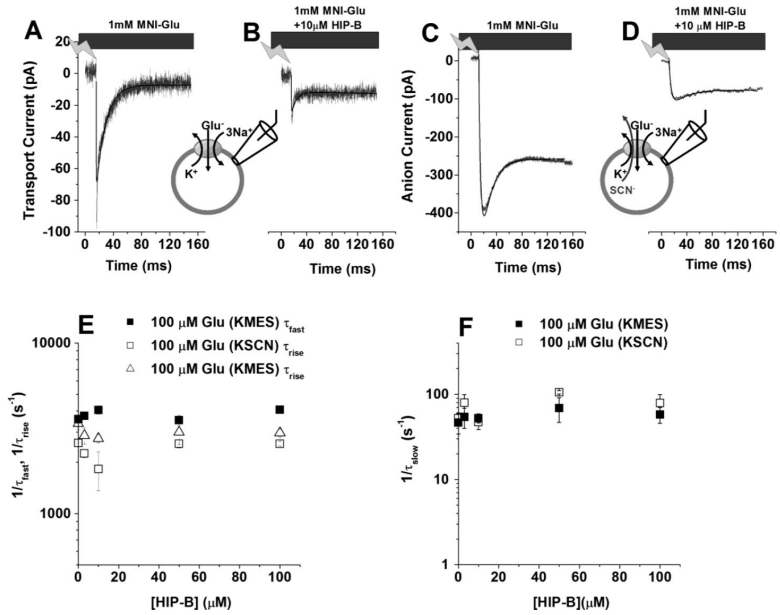


**Figure 6.**

(+)-HIP-B inhibits pre-steady-state current, but not the rate of current relaxations. **(A, B)** Transport current response to rapid release of glutamate from1 mM MNI-caged L-glutamate at the time indicated by the arrow in the absence (A) and presence (B) of 10 μM (+)-HIP-B. The extracellular solution contained 140mM NaMES. The pipette solution contained 140 mM KMES. The solid lines represent a fit with a two-term exponential function. **(C, D)** Experiment under conditions similar as in (A, B), but in the anion conducting mode. The intracellular solution consisted of 140 mM KSCN. The extracellular solution contained 140 mM NaMES. The current traces were fitted with a two-term exponential function. The membrane potential was held at 0 mV in (A–D). **(E)** Observed first-order rate constants for the rapidly-relaxing component as a function of [(+)-HIP-B] in the anion-conducting (open squares) and transport mode (closed squares) as well as the rapid rise component in the transport mode (open triangles). The plot is shown at 100 μM [L-Glu]. **(F)** Observed first order relaxation rate constants for the slowly-decaying component as a function of [(+)-HIP-B] in the anion-conducting (open squares) and transport mode (closed squares). Conditions were the same as in (E).

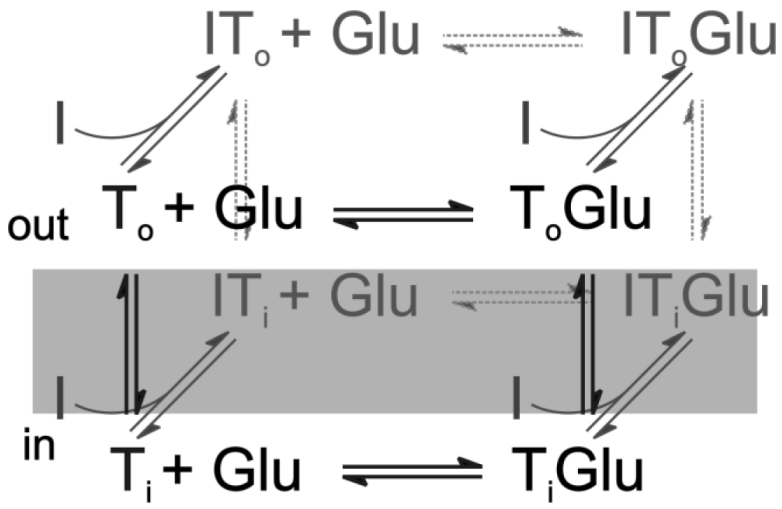


**Figure 7.**

Proposed mechanism of inhibition of the glutamate transporter by (+)-HIP-B (I). $T_o$ and $T_i$ represent the transporter with outward and inward-facing binding sites, respectively. Glu denotes the transported substrate, glutamate. According to the proposed mixed inhibition mechanism, (+)-HIP-B can interact with all configurations of the transporter, although binding to the inward-facing conformation is strongest.

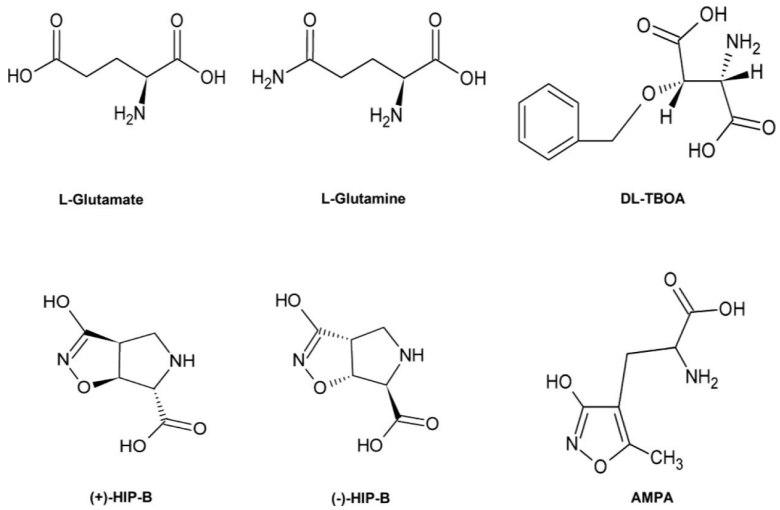


**scheme 1.**

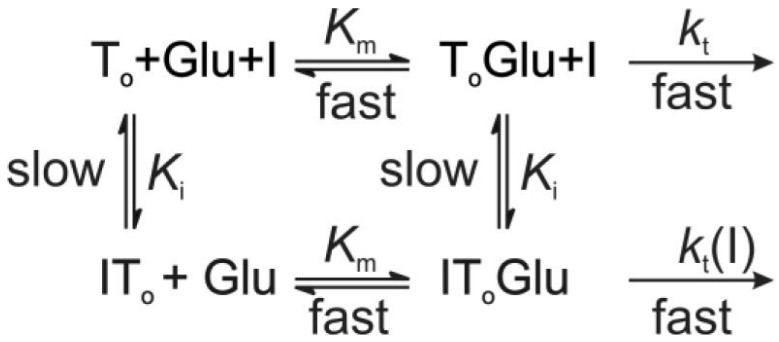


**scheme 2.**